Direct Test of Laser Tunneling with Electron Momentum Imaging

L. Arissian,[1,2] C. Smeenk,[1] F. Turner,[1,3] C. Trallero,[1] A. V. Sokolov,[2] D. M. Villeneuve,[1] A. Staudte,[1] and P. B. Corkum[1]

[1]*Joint Laboratory for Attosecond Science, University of Ottawa and National Research Council,*
100 Sussex Drive, Ottawa K1A 0R6, Canada
[2]*Department of Physics, Texas A & M University, College Station, Texas 77843, USA*
[3]*Department of Physics, University of Waterloo, Waterloo N2L 3G1, Canada*
(Received 9 April 2010; published 24 September 2010)

Tunneling is often used to describe multiphoton ionization of rare gas atoms in infrared fields. We test the tunneling approximation and its nonadiabatic extension by measuring the unperturbed momentum distribution along the *k* direction of a circularly polarized light pulse. We find substantial, but not total, agreement between our results and the predictions of the model. As predicted, the *k* direction momentum distribution is Gaussian and its width increases with the square root of electric field strength. However, the width is 15% too large and we find no evidence of nonadiabatic effects as we approach the expected limits of the approximation.

Tunneling is a quintessential quantum mechanical process with no classical analogue. Introduced to describe essentially time-independent phenomena such as nuclear decay [1], tunneling has proven extremely successful in quantitatively predicting total ionization probabilities of atoms or molecules in intense infrared laser pulses (e.g., [2]). However, in linearly polarized light at 800 nm, the electric field changes from zero to its maximum value and back in less than 2 fs. Hence, the validity of tunneling at optical frequencies has been questioned theoretically [3,4]. Recently, measurements of photoelectron energies have raised additional doubts [5]. On the other hand, angular streaking experiments suggest that tunneling is instantaneous compared to the time scale of optical frequencies [6], and fully differential photoelectron distributions have been qualitatively interpreted by tunneling theory as an image of the orbital from which the electron emerged [7].

To shed more light on this debate we perform a quantitative comparison of tunneling theory with experiment. We measure the intensity and wavelength dependence of photoelectron momentum distributions of single ionization of Ar and Ne using circularly polarized laser pulses. We find that the photoelectron momentum perpendicular to the laser field follows a Gaussian distribution whose width scales with intensity as predicted. The absolute width is in substantial, albeit not total, agreement with tunneling models. Our measured lateral expansion of the electron wave packet is $\approx 15\%$ larger than predicted. To test if this deviation arises from nonadiabatic corrections we have also repeated the experiment at different frequencies. In adiabatic tunnelling the laser field is treated as if it were a static field, time serving only as a parameter. It is rigorously valid for long wavelengths ($\gamma \ll 1$). Nonadiabatic tunnelling refers to deviations that arise at higher frequencies—when the field variation becomes too fast. We do not observe the wavelength scaling predicted by nonadiabatic tunneling [8,9]. In

fact, for the same laser intensity we measure the same width for electrons that tunnel at 800 and 1400 nm.

A rigorous test of the tunneling approximation must disentangle the influence of recollisions [10]—both low impact parameter recollisions and the multiple large impact parameter collisions that comprise Coulomb focusing [11]. Coulomb focusing modifies the lateral momentum distribution in linearly polarized light [12,13] and it is essential to include it in a quantitative description of nonsequential double ionization [14]. As illustrated in Fig. 1(a), an electron that ionizes in circularly polarized light does not reencounter its parent ion. After tunneling, the electron momentum distribution cannot be modified in the direction perpendicular to the plane of polarization. By measuring the perpendicular distribution we observe the nascent quantum mechanical uncertainty in momentum imposed by the tunnel. Circularly polarized light has two other major advantages. First, the large angular momentum suppresses resonantly enhanced multiphoton processes. Second, the field strength at which the electron tunnels can be measured via the momentum it gains in the plane of polarization [Fig. 1(b) side profile] [15]. We will show that the accuracy in field measurement is enhanced by including the initial momentum distribution of the tunneled electron.

We use velocity map imaging (VMI) [16] to record a two-dimensional projection of the three-dimensional photoelectron momentum distribution. For our measurements we used 15 fs 800 nm pulses from a Ti:sapphire laser system [17]; and 70 fs 1400 nm pulses from an optical parametric amplifier. The beams were focused with an on-axis parabolic mirror with $f = 5$ cm (f number 12.5 for 800 nm and f number 20 for 1400 nm). To ensure that the divergence of the focused beam did not influence our results, we performed experiments with different diameter beams (not shown). Our simulations [18] confirm that our results are not influenced by the changes in wave front curvature in the
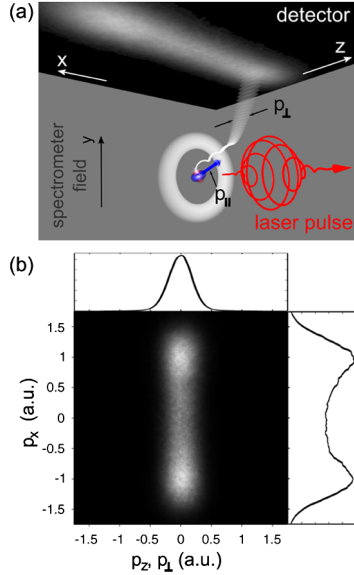
FIG. 1 (color online).   (a) Schematic trajectory of the tunneled electron in circularly polarized light. The drift momentum of the electrons in the plane of laser polarization, summed over possible angles of the ionization field, yields a toroidal distribution of momentum where the center of the ring is E/ω_L. The thickness of this distribution perpendicular to the laser polarization is the width of the momentum distribution at ionization. (b) Measured momentum spectrum of Ar photo electron in circularly polarized light at an intensity of 3.1×10^{14} W/cm^2, 800 nm. The laser propagates along the z axis. The integrated profile along the direction of propagation (top) is in good agreement with a Gaussian distribution. The integrated profile in the plane of polarization (side) is used to determine the intensity.

focus (k distribution) [19]. Details of the system and our calibration procedure are described in [18].

We now turn to the predictions that we test. The idea that tunneling could describe multiphoton ionization for long wavelength or high intensity pulses was introduced by Keldysh [20]. Using only three observables, i.e., the light frequency ω_L, the laser electric field E, and the particle's binding energy I_p, Keldysh introduced a parameter $\gamma = (2I_p)^{1/2}\omega_L/E$ (in atomic units, abbreviated a.u.)—now known as the Keldysh parameter. If $\gamma \ll 1$ multiphoton ionization is approximated by tunneling. If $\gamma \gg 1$, the perturbative description of multiphoton ionization is appropriate. Here, we will present results covering a range of Keldysh parameters from $\gamma = 0.58$ to $\gamma = 1.53$.

A widely used model that describes the tunneling rate for atoms was introduced in the 1980's [21]. Known as the ADK model(for Ammosov, Delone, and Krainov), it predicts the ionization rate W in circularly polarized light scales as (in atomic units) [22,23]

$$W \propto \exp\left(-\frac{2(2I_p)^{3/2}}{3E}\right). \tag{1}$$

Equation (1) assumes the perpendicular momentum of the tunneled electron is negligible. Any nonzero momentum of

the tunneled electron perpendicular to the laser polarization $p_\perp$, can be interpreted as having effectively a higher I_p and less chance for ionization [24,25]. A first-order exponential expansion of the modified I_p results in a Gaussian distribution of $p_\perp$ centered at zero. Including the role of the initial bound state, we obtain the following expression for the perpendicular momentum distribution [26],

$$|\psi_\perp|^2 \propto |\psi_{0\perp}|^2 \exp\left(-p_\perp^2 \frac{\sqrt{2I_p}}{E}\right). \tag{2}$$

Here, $\psi_{0\perp}$ is the momentum space electron wave-function projected perpendicular to the laser polarization. The Gaussian term acts like a filter function on the initial $\psi_{0\perp}$ [7]. The measurable momentum distribution is predicted to have the form $\exp(-p_\perp^2/\sigma^2)$, where $\sigma^2 = E/\sqrt{2I_p}$.

It follows from the tunnel ionization rate that electrons predominantly ionize from orbitals aligned along the polarization axis [23]. This has been confirmed by experiment [27]. Equation (2) shows that, for a given I_p, the width is the same in the plane of polarization and along the k direction [26]. We use the fact that the momentum distribution along the k direction is unaffected by the laser field and we measure it directly. In the plane of polarization, however, the free electron is driven along a classical trajectory by the strong laser field [10]. For long times after the laser pulse has disappeared, the distribution in this direction is centered at $p_\| = E/\omega_L$ [28] [Fig. 1(a)].

A typical image of the momentum distribution of electrons is presented in Fig. 1(b). The laser beam propagation is along z, and x is in the plane of polarization. Integrating the image along the polarization axis (top profile) leads to a Gaussian profile which is used to test Eq. (2). The integrated signal along the propagation axis (side profile) is used to extract the laser field value E at the moment of ionization.

The connection between the momentum distribution of the ions and the laser electric field at the moment-of-birth has been used before to estimate the laser field [15,28]. To improve the fit to the measured electron momentum spectrum [Fig. 2(a)] it is necessary to include the initial quantum distribution of the electron in the plane of polarization. The agreement between the measurement and calculation is evidence that the initial distribution is important.

The data in Fig. 2(a) were taken at approximately the saturation intensity for argon. For the geometry of a focused Gaussian beam, the interaction region can be divided into infinitesimal shells of constant intensity [15]. Since the pulse is short the atoms are essentially stationary during interaction with the laser and the electrons remain in the focus. As the laser pulse develops in time, the number of electrons from a particular geometrical shell varies with time. Saturation effects for single ionization are included in this model; higher order ionization is negligible for the intensities used in this experiment. The only fit parameters in the model are the laser intensity and total electron yield. Our model provides the differential electron yield
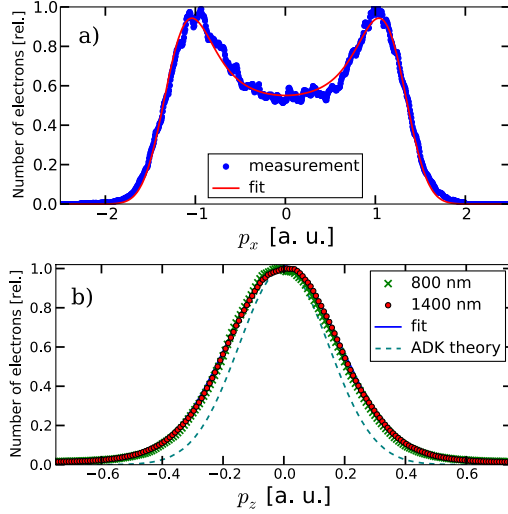
FIG. 2 (color online). (a) Measured and calculated distribu-
tions at 3.2×10^{14} W/cm^2, integrated along the propagation
axis. The quality of the fit to data is significantly improved by
including the momentum distribution of tunneled electrons in
our algorithm. (b) The electron wave packet at 800 and 1400 nm
is shown along the p_z axis. The laser intensity was 1.8×10^{14} W/cm^2 for both wavelengths. Also shown is a Gaussian
fit to the measurement and the prediction of the ADK theory
[Eq. (2)] at this intensity. The small offset of the center from zero
is due to photon linear momentum [33].

distribution in the focus, dN/dE where N is the relative
number of electrons and E is the laser field. For simplic-
ity in plotting the data we attributed a value of $E_{\mathrm{avg}} = \int_0^{E_0} E \frac{dN}{dE} dE$ to each distribution where E_0 is the peak elec-
tric field. To a large extent $E_{\mathrm{avg}} \approx E_0$ for a pulse below the
saturation intensity. For a pulse with peak intensity above
the saturation limit $E_{\mathrm{avg}} \approx E_{\mathrm{sat}}$ (that is, the field where
approximately 40% of the particles are ionized [29]).

Our experiment is in the regime $\gamma \approx 1$ so it is not clear
that the electron can adiabatically follow the oscillating
laser field. This is one assumption at the core of tunneling
theory. Incorporating corrections for nonadiabatic effects
introduces a wavelength dependence to the tunneling rate
[8] and electron momentum spectrum [9].

For direct comparison with Eq. (2) we have included the
bound momentum distribution in the nonadiabatic theory.
The bound electron distribution $|\psi_{0\perp}|^2$ is used to multiply
Eq. (8) in Ref. [9]. In the nonadiabatic theory the momen-
tum distribution scales with the laser wavelength as shown
in the dashed curves of Fig. 3(a).

The measurement of the wave packet width as a function
of laser field in argon for both 800 and 1400 nm is pre-
sented in Fig. 3(a). The data are plotted against predictions
of Eq. (2) and the nonadiabatic theory. There is a substan-
tial agreement between our data and the predictions of
tunneling models. However, a deviation of about 15%
remains. Our result shows that the width of the distribution
perpendicular to the tunnel is only a function of the laser
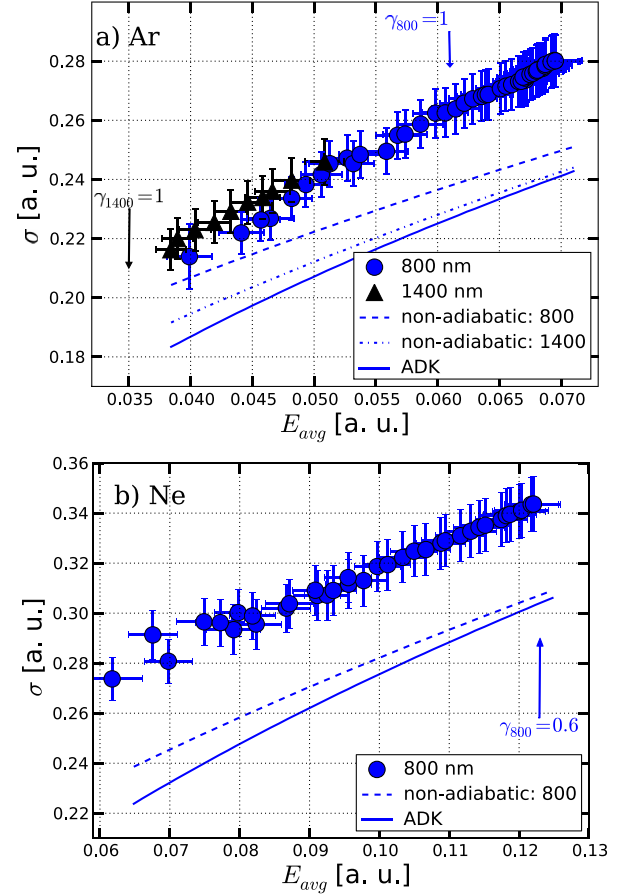field and not the laser wavelength. The error bars include

FIG. 3 (color online). (a) Width σ of the momentum distribu-
tion as a function of average laser field in the focus for argon at
800 and 1400 nm. The data are compared with predictions of
nonadiabatic and ADK theories. (b) Width of the momentum
distribution as a function of the field for neon.

uncertainties in detector response, alignment and momen-
tum calibration of the spectrometer, laser ellipticity, and
numerical accuracy of the fit.

A similar result is obtained for neon in Fig. 3(b). The
width of the distribution expands with increase in laser
field, however both existing theories predict different
values for the absolute width of the measurement.

When we began this experiment we expected a major
change in σ as ionization left the tunneling regime
[30–32]. To test this hypothesis we used the second har-
monic of the 800 nm pulse to ionize argon. The 400 nm,
50 fs pulse was also circularly polarized ($\gamma \sim 2.5$). While
400 nm ionization of argon is outside the region where
tunneling is expected to be a valid approximation, we still
measure a profile with a width that is similar to the values
in the infrared. An example of a measured distribution for
argon at 400 nm is shown in Fig. 4 where the inset is the
measured 2D spectrum and the figure is integrated over p_x.
At this wavelength it was not possible to use the same
intensity measurement method as in the infrared. We
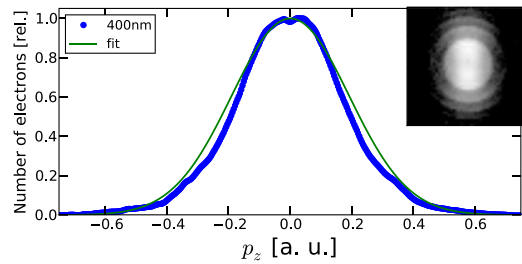scanned the intensity over an estimated range 5×10^{13} W/cm^2 to 5×10^{14} W/cm^2. While the total electron

FIG. 4 (color online). Integrated lateral distribution from ionization of Ar at 400 nm using circularly polarized light at approximately 2×10^{14} W/cm^2. Inset shows the measured 2D electron distribution (log color scale).

yield increased substantially with intensity, we found no systematic intensity dependence of the lateral profile. Additionally, the width of the lateral distribution lies in the same range as the measurements in the infrared. The peak intensity used for the measurement in Fig. 4 is estimated as $(2 \pm 1) \times 10^{14}$ W/cm^2. The large uncertainty in the intensity arises from the combined uncertainty in the pulse duration and focal spot size.

In conclusion, the relation between the lateral and longitudinal momentum from tunneling models is accurate when circularly polarized light is used. This is very important. Tunneling is one of the simplest of quantum mechanical phenomena. It has the robustness on which technologies are built. If laser experiments are accurately described by tunneling, then multiphoton ionization becomes a reliable tool to probe molecules, much like an STM probes solids.

Our results imply there may be a deeper question that has not been explored. Is there a fundamental reason why the lateral momentum distribution is insensitive to the light wavelength for $0.58 \leq \gamma \leq 1.53$? We have shown that the experimental electron distribution for circularly polarized light is relatively consistent with tunnelling models. This contrasts with linear polarized experiments where significant deviations have been reported. We note that both experiments share the tunnelling step, but recollision only occurs for linear polarization.

[1] G. Gamow, Z. Phys. **51**, 204 (1928).
[2] B. Walker, B. Sheehy, L. F. DiMauro, P. Agostini, K. J. Schafer, and K. C. Kulander, Phys. Rev. Lett. **73**, 1227 (1994).
[3] H. R. Reiss, Phys. Rev. Lett. **101**, 043002 (2008).
[4] H. R. Reiss, Phys. Rev. Lett. **102**, 143003 (2009).
[5] C. Blaga, F. Catoire, P. Colisimo, G. Paulus, H. Muller, P. Agostini, and L. DiMauro Nature Phys. **5**, 335 (2009).
[6] P. Eckle, A. N. Pfeiffer, C. Cirelli, A. Staudte, R. Dorner, H. Muller, M. Buttiker, and U. Keller, Science **322**, 1525 (2008).
[7] M. Meckel, D. Comtois, D. Zeidler, A. Staudte, D. Pavicic, H. C. Bandulet, H. Pepin, J. C. Kieffer, R. Dorner, D. M. Villeneuve, and P. B. Corkum, Science **320**, 1478 (2008).
[8] G. Yudin and M. Y. Ivanov, Phys. Rev. A **64**, 013409 (2001).
[9] D. I. Bondar, Phys. Rev. A **78**, 015405 (2008).
[10] P. B. Corkum, Phys. Rev. Lett. **71**, 1994 (1993).
[11] T. Brabec, M. Y. Ivanov, and P. B. Corkum, Phys. Rev. A **54**, R2551 (1996).
[12] D. Comtois, D. Zeidler, H. Pepin, J. C. Kieffer, D. M. Villeneuve, and P. B. Corkum, J. Phys. B **38**, 1923 (2005).
[13] A. Rudenko, K. Zrost, Th Ergler, A. B. Voitkiv, B. Najjari, V. L. B. de Jesus, B. Feuerstein, C. D. Schroter, R. Moshammer, and J. Ullrich, J. Phys. B **38**, L191 (2005).
[14] G. L. Yudin and M. Y. Ivanov, Phys. Rev. A **63**, 033404 (2001).
[15] A. S. Alnaser, X. M. Tong, T. Osipov, S. Voss, C. M. Maharjan, B. Shan, Z. Chang, and C. L. Cocke, Phys. Rev. A **70**, 023413 (2004).
[16] A. Eppink and D. Parker, Rev. Sci. Instrum. **68**, 3477 (1997).
[17] M. Nisoli, S. De Silvestri, O. Svelto, R. Szipocs, K. Ferencz, Ch. Spielmann, S. Sartania, and F. Krausz, Opt. Lett. **22**, 522 (1997).
[18] See supplementary material at http://link.aps.org/supplemental/10.1103/PhysRevLett.105.133002.
[19] F. L. Pedrotti and S. J. Pedrotti, *Introduction to Optics* (Prentice-Hall, Englewood Cliffs, NJ, 1993), 2nd ed.
[20] L. V. Keldysh, Sov. Phys. JETP **20**, 1307 (1965).
[21] M. V. Ammosov, N. B. Delone, and V. P. Krainov, Sov. Phys. JETP **64**, 1191 (1986).
[22] N. B. Delone and V. P. Krainov, Phys. Usp. **41**, 469 (1998).
[23] N. B. Delone and V. P. Krainov, *Multiphoton Processes in Atoms* (Springer-Verlag, Berlin, 2000), 2nd ed.
[24] N. B. Delone and V. P. Krainov, J. Opt. Soc. Am. B **8**, 1207 (1991).
[25] A. M. Perelomov, V. S. Popov, and M. V. Terentev, Sov. Phys. JETP **24**, 207 (1967).
[26] M. Ivanov, M. Spanner, and O. Smirnova, J. Mod. Opt. **52**, 165 (2005).
[27] D. Shafir, Y. Mairesse, D. M. Villeneuve, P. B. Corkum, and N. Dudovich, Nature Phys. **5**, 412 (2009).
[28] I. V. Litvinyuk, K. F. Lee, P. W. Dooley, D. M. Rayner, D. M. Villeneuve, and P. B. Corkum, Phys. Rev. Lett. **90**, 233003 (2003).
[29] S. M. Hankin, D. M. Villeneuve, P. B. Corkum, and D. M. Rayner, Phys. Rev. A **64**, 013405 (2001).
[30] V. Schyja, T. Lang, and H. Helm, Phys. Rev. A **57**, 3692 (1998).
[31] P. Kaminski, R. Wiehle, V. Renard, A. Kazmierczak, B. Lavorel, O. Faucher, and B. Witzel, Phys. Rev. A **70**, 053413 (2004).
[32] C. M. Maharjan, A. Alnaser, I. V. Litvinyuk, P. Ranitovic, and C. L. Cocke, J. Phys. B **39**, 1955 (2006).
[33] C. Smeenk, L. Arissian, B. Zhou, A. Mysyrowicz, D. M. Villeneuve, A. Staudte, and P. B. Corkum (to be published).